INSTITUTE OF PHYSICS PUBLISHING SEMICONDUCTOR SCIENCE AND TECHNOLOGY
Semicond. Sci. Technol. **17** (2002) R21–R34 PII: S0268-1242(02)25015-4

TOPICAL REVIEW

Coulomb drag between ballistic one-dimensional electron systems

P Debray[1], V N Zverev[2], V Gurevich[3], R Klesse[4] and R S Newrock[5]

[1] Service de Physique de lÉtat Condensé, CEA Saclay, 91191 Gir-sur-Yvette, France
[2] Institute of Solid State Physics RAS, Chemogolovka, Moscow region, 142432, Russia
[3] Solid State Physics Division, A F Ioffe Institute, 194021 Saint Petersburg, Russia
[4] Institut für Theoretische Physik, Universität zu Köln, Germany
[5] Department of Physics, University of Cincinatti, OH 45221-0011, USA

Received 19 July 2002
Published 16 October 2002
Online at stacks.iop.org/SST/17/R21

Abstract
The presence of pronounced electronic correlations in one-dimensional systems strongly enhances Coulomb coupling and is expected to result in distinctive features in the Coulomb drag between them that are absent in the drag between two-dimensional systems. In this review, we review recent Fermi and Luttinger liquid theories of Coulomb drag between ballistic one-dimensional electron systems, also known as quantum wires, in the absence of inter-wire tunnelling, to focus on these features and give a brief summary of the experimental work reported so far on one-dimensional drag. Both the Fermi liquid (FL) and the Luttinger liquid (LL) theory predict a maximum drag resistance R_D when the one-dimensional subbands of the two quantum wires are aligned and the Fermi wave vector k_F is small, and also an exponential decay of R_D with increasing inter-wire separation, both features confirmed by experimental observations. A crucial difference between the two theoretical models emerges in the temperature dependence of the drag effect. Although the FL theory predicts a linear temperature dependence, the LL theory promises a rich and varied dependence on temperature depending on the relative magnitudes of the energy and length scales of the systems. At very low temperatures, the drag resistance may diverge due to the formation of locked charge density waves. At higher temperatures, it should show a power-law dependence on temperature, $R_D \propto T^x$, experimentally confirmed in a narrow temperature range, where x is determined by the Luttinger liquid parameters. The spin degree of freedom plays an important role in the LL theory in predicting the features of the drag effect and is crucial for the interpretation of experimental results. Substantial experimental and theoretical work remains to be done for a comprehensive understanding of one-dimensional Coulomb drag.

1. Introduction

Moving charge carriers in a conductor exert a Coulomb force on the charge carriers in a nearby conductor and induce a drag current in the latter via momentum transfer. This phenomenon, known as Coulomb drag, was predicted by Pogrebinskii in his pioneering paper [1] in which he argued that in a structure of two semiconductor layers separated by an insulating layer, there would be a drag of carriers in layer 1 ('drag layer'), resulting in a drag current I_D, due to the direct Coulomb interaction with the carriers in layer 2 ('drive layer'), where an electric current I flows. If no current is allowed to flow in

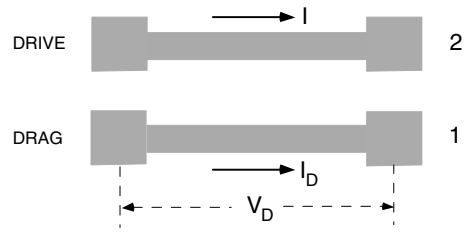

Figure 1. Schematic view of Coulomb drag between parallel quantum wires.

the drag layer, the charge carriers will accumulate at one end inducing a charge imbalance across the layer. This charge will continue to accumulate until the force of the resulting electric field balances the drag force. In the stationary state there will be an induced or 'drag' voltage V_D in the drag layer. When the carriers in both layers are of the same type (electrons or holes), the drag voltage has a sign opposite to the voltage drop in the drive layer. Figure 1 gives a schematic view of Coulomb drag between two parallel quantum wires. The quantity usually measured in experiments is the drag voltage V_D. The drag resistance R_D is defined as $R_D = -V_D/I$.

Coulomb drag between two-dimensional (2D) electron systems has been extensively studied [2] both experimentally and theoretically. The basic physics involved in the description of the drag in two dimensions is now well understood on the basis of Fermi liquid (FL) theory of interacting fermions. The FL theory is well established in three dimensions and holds marginally for many two-dimensional systems, but generally fails in one dimension. The theory is based on Landau's conjecture that the low-lying excitations of interacting fermion systems can be connected continuously to those of the non-interacting Fermi gas—there is a smooth mapping between the quasiparticles of the interacting and those of the non-interacting system [3].

Coulomb drag between one-dimensional (1D) electron systems has been the focus of considerable interest in recent years because our understanding of the quantum properties in interacting 1D systems is unsatisfactory. Experimental work on the subject remains quite limited [4–7]; however, a fair number of theoretical papers have been published [8–18]. The primary reason for this theoretical interest is that Coulomb drag is one of the most effective ways to study electron–electron (*e–e*) interaction.

It is now theoretically established that in an interacting 1D electron gas of infinite length, the *e–e* interaction completely modifies the ground state of the system. The elementary excitations cannot be treated as non-interacting quasiparticles of a conventional Fermi liquid, but instead acquire a bosonic nature. An adequate theoretical description of these interacting 1D systems can be given in terms of the so-called Luttinger liquid (LL) [19] (for a recent review see [20]), complementary to the FL description in higher dimensions. In a real 1D system of finite length at finite temperatures, the extent of influence of the *e–e* interaction will depend on the system parameters.

Experimental details to observe the manifestation of Luttinger liquid behaviour, however, have been quite limited [21–24]. Part of the problem is that the (*e–e*) interaction has little influence on the conductance of a single wire, since the current is proportional to the total electron quasi-momentum, which is conserved in electron–electron collisions. To look for experimental evidence of the LL state, it would therefore help to explore a new experimental tool based on new devices and physical phenomena. Coulomb drag between 1D electron systems in a dual-wire configuration opens up a new opportunity and avenue for experimentally probing the LL state in a 1D electron system.

The purpose of this review is to present the current status of the theory of Coulomb drag between 1D electron systems for electron transport in the ballistic regime, and to report on experimental measurements of the 1D drag effect. Ballistic transport takes place when the quantum wire dimensions are smaller than both the elastic and the inelastic scattering lengths. Electron transport is strictly one dimensional when only the lowest 1D subband of the wire is occupied and transport takes place in the fundamental mode. The ballistic regime is well suited for Coulomb drag study, since in this regime other scattering processes, such as impurity and phonon scattering, are either insignificant or totally absent.

Further theoretical and experimental investigation of the 1D Coulomb drag effect can enhance our general understanding of the properties of systems of low dimensionality. This broad class of systems is currently a very active area of research. In addition to its fundamental interest, a comprehensive understanding of Coulomb interaction between quantum wires is expected to play a significant role in the design of nanodevices, such as single-electron transistors (SETs) [25] and quantum cellular automata (QCA) [26], which are composed of quantum dots and quantum wires in close proximity.

The paper is organized as follows: Section 2 describes the theory of 1D Coulomb drag based on the Fermi liquid approach. Section 3 reviews the Luttinger liquid description of this effect. In section 4 we present a summary of the experimental work reported so far and a comprehensive analysis of the experimental results using both the FL and the LL descriptions of 1D Coulomb drag. Finally, section 5 gives some guidelines for future work on the subject.

2. Fermi liquid approach

In this section the 1D Coulomb drag is analysed within the Fermi liquid concept. We will follow [8, 18] and use the physical picture developed by Landauer [27], Imry [28] and Büttiker [29]. We assume that each quantum wire is connected to ideal electronic reservoirs attached to its ends. The relaxation processes in the reservoirs are considered to be so fast that each of them is in thermal equilibrium.

The *e–e* interaction within a single quantum wire does not result in a current variation because of the quasimomentum conservation in the *e–e* collisions. However, if two such wires, 1 and 2, are near one another and parallel, the Coulomb interaction of electrons belonging to different wires can transfer momenta between the wires, which eventually gives rise to a drag effect.

The drag force due to the ballistic current in wire 2 creates a sort of permanent acceleration on the electrons of wire 1. As wire 1 has a finite length L a steady drag current I_D is established.

Within the Fermi liquid approach we restrict ourselves to direct electron–electron collisions mediated by the Coulomb

interaction. Let us analyse the conservation laws for such collisions of electrons belonging to two different wires, 1 and 2, each of them being parallel to the x-axis. We have

$$\epsilon^{(1)}_{nk} + \epsilon^{(2)}_{n'k'} = \epsilon^{(1)}_{l,k+q} + \epsilon^{(2)}_{l',k'-q}. \tag{1}$$

Here $\hbar k$ is the x-component of the electron quasimomentum. In this and the next sections we will put $\hbar = 1$ and $k_B = 1$ (where k_B is the Boltzmann constant). These quantities will be restored only in some final (or most important) formulae. Now,

$$\epsilon^{(1,2)}_{nk} = \varepsilon^{(1,2)}_{n}(0) + k^2/2m, \tag{2}$$

m being the effective mass while n being the transverse quantization subband (channel) index, with primed quantities corresponding to wire 2 throughout. The solution of equation (1) can be written as

$$q = -(k-k')/2 \pm \sqrt{(k-k')^2/4 + m\delta\varepsilon} \tag{3}$$

with $\delta\varepsilon = \varepsilon^{(1)}_{n}(0) + \varepsilon^{(2)}_{n'}(0) - \varepsilon^{(1)}_{l}(0) - \varepsilon^{(2)}_{l'}(0)$.

We assume that the electrons of the quantum wires are degenerate and the temperature is low compared to the electron Fermi energy. For the electron–electron collision to be possible, the absolute values of the four quantities, namely, $\epsilon^{(1)}_{nk}$, $\epsilon^{(2)}_{n'k'}$, $\epsilon^{(1)}_{l,k+q}$ and $\epsilon^{(2)}_{l',k'-q}$ should be within the stripes k_BT near the corresponding Fermi levels. This means that within the accuracy mT/k_F, the following relations should be valid

$$\begin{aligned} k &= k^{(n)}_F, & k' &= k^{(n')}_F, \\ |k+q| &= k^{(l)}_F, & |k'-q| &= k^{(l')}_F. \end{aligned} \tag{4}$$

Here $k^{(n)}_F$ denotes the Fermi quasimomentum for band n. In general it is impossible by variation of a single quantity, i.e. the transferred quasimomentum q, to satisfy both relations of equation (4) (provided, of course, that the distances between the channel bottoms are much bigger than T).

In other words, one cannot in general satisfy equation (1) for a finite $\delta\epsilon$. Therefore for a general case one should have $n = l, \quad n' = l'$. If both wires are identical equations $n = l', \quad n' = l$ are also possible. In both cases $\delta\epsilon = 0$. We will assume the wires to be different. Then

$$\delta\left(\epsilon^{(1)}_{nk} + \epsilon^{(2)}_{n'k'} - \epsilon^{(1)}_{l,k+q} - \epsilon^{(2)}_{l',k'-q}\right) = (m/|q|)\delta(k-k'+q). \tag{5}$$

This means that the quasimomentum transferred during a collision is $q = k' - k$, i.e. the electrons swap their quasimomenta as a result of collision.

Assuming that the drag current in wire 1 is much smaller than the ballistic current in wire 2, we calculate the drag current by solving the Boltzmann equation for wire 1 (otherwise we should have solved a system of coupled equations for both wires). We assume the wires to be different though having the same lengths L and consider the interaction processes when electrons in the two quantum wires after scattering remain within the initial subbands $\epsilon^{(1)}_{nk} = \varepsilon^{(1)}_{n}(0) + k^2/2m$ and $\epsilon^{(2)}_{n'k} = \varepsilon^{(2)}_{n'}(0) + k^2/2m$, n being the subband's number. The Boltzmann equation for the electrons occupying the nth subband is

$$v_k \frac{\partial F^{(1)}}{\partial k} = \mathcal{I}^{(12)}\{F^{(1)}, F^{(2)}\} \tag{6}$$

where $F^{(1,2)}$ are the electron distribution functions in wires 1 and 2 respectively, and $\mathcal{I}$ is the collision integral. We assume that the only type of collisions that is essential is the inter-wire e–e collisions described by the term

$$\mathcal{I}^{(12)}\{F^{(1)}, F^{(2)}\} = 2\int \frac{dk'}{2\pi}\int \frac{dq}{2\pi}\sum_{n'} w(1, k+q, n; 2, k'-q, n' \leftarrow 1, k, n; 2, k', n')\mathcal{P} \tag{7}$$

where

$$\mathcal{P} = \left[F^{(1)}_{nk}F^{(2)}_{n'k'}\left(1 - F^{(1)}_{nk+q}\right)\left(1 - F^{(2)}_{n'k'-q}\right) - F^{(1)}_{nk+q}F^{(2)}_{n'k'-q}\left(1 - F^{(1)}_{nk}\right)\left(1 - F^{(2)}_{n'k'}\right)\right], \tag{8}$$

2 is the spin factor; the scattering probabilities are assumed to be spin-independent. If the e–e collisions can be treated within the perturbation theory, then the scattering probability is given by

$$\begin{aligned} &w(1, k+q, n, 2, k'-q, n' \leftarrow 1, k, n; 2, k', n') \\ &\quad = 2\pi|\langle 1, k+q, n; 2, k'-q, n'|V|1, k, n; 2, k', n'\rangle|^2 \\ &\qquad \times \delta\left(\epsilon^{(1)}_{nk} + \epsilon^{(2)}_{n'k'} - \epsilon^{(1)}_{n,k+q} - \epsilon^{(2)}_{n',k'-q}\right). \end{aligned} \tag{9}$$

The matrix element of electron–electron interaction can be transformed to

$$\begin{aligned} &\langle 1, k+q, n; 2, k'-q, n'|V|1, k, n; 2, k', n'\rangle \\ &\quad = \frac{1}{L}\int d^2r_\perp \int d^2r'_\perp \phi^*_n(\mathbf{r}_\perp)\phi^*_{n'}(\mathbf{r}'_\perp) \\ &\qquad \times V_q(\mathbf{r}_\perp - \mathbf{r}'_\perp)\phi_n(\mathbf{r}_\perp)\phi_{n'}(\mathbf{r}'_\perp) \end{aligned} \tag{10}$$

where $V_q = \int dx\, V(x, \mathbf{r}_\perp)\exp(-iqx)$, $\mathbf{r}_\perp = (y, z)$. We have

$$\int dx \int dx' V(\mathbf{r} - \mathbf{r}')\, e^{iq(x-x')} = 2e^2 L K_0(|q\|\Delta r_\perp|) \tag{11}$$

where $\Delta\mathbf{r}_\perp = \mathbf{r}_\perp - \mathbf{r}'_\perp$ and K_0 is a modified Bessel function defined in [30]. Now,

$$K_0(\xi) = \begin{cases} -\ln(\xi/2) & \xi \ll 1, \\ \sqrt{\pi/2\xi}\, e^{-\xi} & \xi \gg 1. \end{cases} \tag{12}$$

It means that the e–e interaction goes down exponentially provided $|q\|\mathbf{r}_\perp - \mathbf{r}'_\perp|/\hbar \gg 1$.

To calculate the current in wire 1, we iterate the Boltzmann equation (6) in the collision term $\mathcal{I}^{(12)}$. The first iteration gives for the nonequilibrium part of the distribution function $\Delta F^{(1)}_{np}$

$$\Delta F^{(1)}_{nk} = -\left(z \pm \frac{L}{2}\right)\frac{1}{v_n}\mathcal{I}^{(12)}\{F^{(1)}, F^{(2)}\} \tag{13}$$

for $k > 0$ ($k < 0$) respectively. One gets for the drag current

$$I_D = -2eL\sum_n \int_0^\infty \frac{dk}{2\pi}\mathcal{I}^{(12)}\{F^{(1)}, F^{(2)}\}. \tag{14}$$

We assume in the spirit of the Landauer–Büttiker–Imry approach the driving wire connected to the reservoirs which we call 'left' (+) and 'right' (−), each of these being in independent equilibrium. Let the x-component of the quasimomentum of an electron in wire 2 before scattering be k' and after scattering by an electron of wire 1 let this be $k' - q$. Let $k' > 0$ while $k' - q < 0$. Then the first distribution function in wire 2 is $F^{(0)}_{n'k} = f\left(\epsilon^{(2)}_{n'k} - \mu^{(+)}\right)$ where f is the equilibrium Fermi function. The second one is $F^{(0)}_{l',k+q} = f\left(\epsilon^{(2)}_{l',k+q} - \mu^{(-)}\right)$ where $\mu^{(\pm)} = \mu \pm eV/2$. At $eV = 0$

the wires are in equilibrium. We denote the corresponding equilibrium chemical potential as μ.

Let us denote by $\Delta\{F\}$ the expression one gets after substitution of the equilibrium distribution functions given above into the collision term. For $k' > 0$ ($k' < 0$) and $k' - q < 0$ ($k' - q > 0$), where k' is the electron quasimomentum in wire 2 before the scattering, we obtain

$$\Delta\{F^{(1)}, F^{(2)}\} = \pm 2 \sinh\left(\frac{eV}{2T}\right)\left[1 - f\left(\epsilon^{(1)}_{nk} - \mu\right)\right] \times \left[1 - f\left(\epsilon^{(2)}_{n',k'} - \mu^{(+)}\right)\right] \times f\left(\epsilon^{(1)}_{n,k+q} - \mu\right) f\left(\epsilon^{(2)}_{n',k'-q} - \mu^{(-)}\right). \quad (15)$$

We begin with a discussion of the ohmic case $eV/k_B \ll 1$. Accordingly, we replace $\sinh(eV/2T)$ by its argument and all the chemical potentials in equation (15) by the same value μ. The initial and final states of the colliding electrons should be within T of the Fermi levels [8]. This means that only the terms with $\varepsilon^{(1)}_n(0) = \varepsilon^{(2)}_{n'}(0)$, where the equality is satisfied with the indicated accuracy, give the principal contribution to the current. (The importance of equal channel velocities was also pointed out in [9].) The contribution of each such pair of levels to the current is

$$I_D = \frac{e^5 m^3 L k_B T e V}{2\pi^2 \kappa^2} \frac{1}{{k_n}^3} g_{nn}(2k_n) \frac{\left[\varepsilon^{(1)}_n(0) - \varepsilon^{(2)}_{n'}(0)\right]^2}{4(k_B T)^2} \times \left[\sinh \frac{\varepsilon^{(1)}_n(0) - \varepsilon^{(2)}_{n'}(0)}{2k_B T}\right]^{-2} \quad (16)$$

where

$$g_{nn'}(q) = \left| \int d^2 r_\perp \int d^2 r'_\perp |\phi_n(r_\perp)|^2 |\phi_n(r'_\perp)|^2 K_0(q|\Delta \mathbf{r}_\perp|) \right|^2, \quad (17)$$

κ is the dielectric susceptibility of the lattice, $k_n = \sqrt{2m[\mu - \varepsilon_n(0)]}$. This equation has also been obtained using linear response theory. In the case considered, wire 2 is a part of a usual structure for measuring ballistic conductance, i.e. it joins two classical reservoirs, each of them being in independent equilibrium. The driving current is [28]

$$I = \mathcal{N} \frac{e^2}{\pi} V, \quad (18)$$

$\mathcal{N}$ being the number of active channels (i.e. the subbands whose bottoms are below the Fermi level). So far a simplifying assumption has been used: the chemical potential μ in wire 1 and the average chemical potential in wire 2 are equal. In the general case they can have different values $\mu^{(1)}$ and $\mu^{(2)}$, respectively. Then one still gets equation (16) with the replacement

$$\varepsilon^{(1,2)}_n(0) \to \tilde{\varepsilon}^{(1,2)}_n(0) \equiv \varepsilon^{(1,2)}_n(0) - \mu^{(1,2)}.$$

One can measure either the current or the voltage that builds up in wire 1. The ratio of the drag current to the ballistic driving current for $\tilde{\epsilon}^{(1)}_n(0) = \tilde{\epsilon}^{(2)}_{n'}(0)$ is given by

$$\frac{I}{I_D} = \frac{4e^4 m^3 L k_B T}{\pi \hbar^3 \kappa^2 \mathcal{N}} \sum_{nn'} \mathcal{D}_{nn'} \quad (19)$$

where

$$\mathcal{D}_{nn'} = \frac{1}{\left(k^{(1)}_n + k^{(2)}_n\right)^3} g_{nn'}\left(k^{(1)}_n + k^{(2)}_n\right). \quad (20)$$

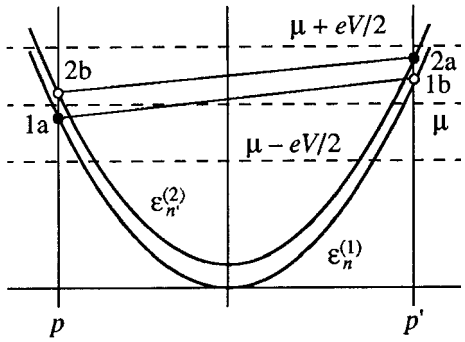

Figure 2. Schematic representation (for $\mu^{(1)} = \mu^{(2)}$) of simultaneous transitions due to the interaction between electrons of the two wires for $eV \gg k_B T$. Circles ○ and • represent the initially unoccupied and occupied states respectively.

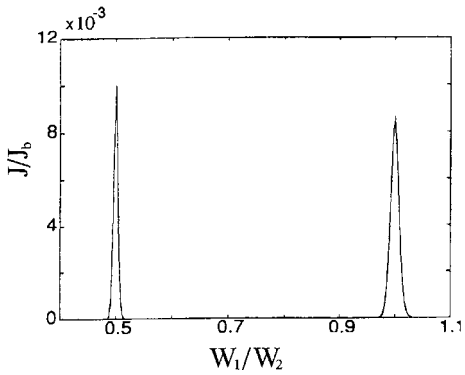

Figure 3. I/I_D is plotted (for $\mu^{(1)} = \mu^{(2)} = \mu$) as a function of W_1/W_2 where the width of wire 1 is controlled through gate voltage ($\mu = 14$ meV, $T = 1$ K, $W_2 = 42$ nm, $L = 1\mu$m, $\kappa = 13$ and the spacing between wires is 50 nm).

Here $k^{(1,2)}_n = \sqrt{2m\left[\mu^{(1,2)} - \varepsilon^{(1,2)}_n(0)\right]}$. In this approximation, $k^{(1,2)}_n = k^{(1,2)}_{n'}$. In an experiment one usually measures the drag resistance $R_D = -V_D/I = I_D G_D/I$, where G_D is the ballistic resistance of the drag wire and depends on the number of occupied subbands.

The 1D subband structure of the wires can be modified by changing the effective wire widths by applying appropriate gate voltages (figure 5). The variation of gate voltage may affect the positions of the levels of transverse quantization in the two wires in a different way. In the course of such a variation, a coincidence of a pair of such levels in the two wires may be reached. The estimate (20) is not very sensitive to the form of confining potential and electron densities. In figure 3 the ratio I/I_D is plotted (for $\mu^{(1)} = \mu^{(2)}$) as a function of the ratio of effective wire widths. This plot exhibits striking oscillations with large peak-to-valley ratios. The peaks occur when channel velocities in two interacting wires are equal which happens whenever any two current-carrying channels line up. This sort of coupling is particularly strong when such channel velocities are quite small.

The condition $\tilde{\epsilon}^{(1)}_n(0) = \tilde{\epsilon}^{(2)}_{n'}(0)$ gives the main maxima of the drag current, especially for the lowest levels of transverse quantization. Some subsidiary maxima can also be observed, particularly in external magnetic field, see [14].

So far we have considered the peaks of the drag current under conditions where the Fermi level is well above the

coinciding bands in wires 1 and 2. Now we would like to say a few words about a special case that may be particularly important regarding the experiment described below. This is the case where the bottoms of two subbands not only coincide but also just touch the Fermi level. Then the conduction electrons obey the so-called *intermediate statistics*. It means that their equilibrium distribution functions are

$$f = \frac{1}{\exp(k^2/2mT) + 1}. \tag{21}$$

The drag current is proportional to the *e–e* scattering probability averaged over this distribution function. The scattering probability itself is determined by the quantum mechanics, i.e. it depends on the form of electron wavefunction in the quantum wire, or in other words, on the exact form of the confining potential. Investigation of the temperature dependence of the drag in this special case is one of the problems of the theory to be solved in future.

Now we turn to the case of non-ohmic transport in the drive wire, i.e. to the case where $eV \gg k_{\mathrm{B}}T$ [18]. The situation for $\mu^{(1)} = \mu^{(2)}$ is illustrated in figure 2. The upper and lower dashed lines correspond to the positions of the chemical potentials $\mu^{(-)}$ and $\mu^{(+)}$, respectively, while the middle dashed line corresponds to the average value μ. Parabolas (1) and (2) represent the dispersion law of electrons in wires 1 and 2 respectively. The full circles correspond to the initial states of colliding electrons.

Before the collision, states 1a and 2a are occupied. The circle representing state 1a is below the dashed line, i.e. below the Fermi level μ. The circle 2a represents a state with $p > 0$, which is also occupied as the corresponding energy is below $\mu^{(+)}$.

After the collision, state 1b is occupied. It is represented by a circle above the dashed line, which means that it has been free before the collision. In wire 2 state 2b with $p < 0$ is also occupied. It is above $\mu^{(+)}$, i.e. it had been free before the transition.

The width of the stripe between the two straight lines is eV. If the bottoms of the active subbands are well below the Fermi level, the drag current should be proportional to the number of occupied initial states as well as to the number of free final states.

To calculate the drag current, one can recast the product of distribution functions in the collision term, equations (7) and (8), into the form

$$\mathcal{P} = 2\sinh(eV/2T)\mathcal{Q} \tag{22}$$

where

$$\mathcal{Q} = \exp\frac{\varepsilon^{(1)}_{nk} - \mu}{T}\exp\frac{\varepsilon^{(2)}_{n'k'} - \mu}{T} f\left(\varepsilon^{(1)}_{nk} - \mu\right) f\left(\varepsilon^{(2)}_{n'k'} - \mu^{(+)}\right) \times f\left(\varepsilon^{(1)}_{nk'} - \mu\right) f\left(\varepsilon^{(2)}_{n'k} - \mu^{(-)}\right). \tag{23}$$

For the drag current one gets

$$I = -\sinh\left(\frac{eV}{2T}\right)\frac{8e^5 mL}{\pi^2\kappa^2}\sum_{nn'}\int_0^\infty \mathrm{d}k\int_0^\infty \mathrm{d}k'\,\frac{g_{nn'}(k+k')}{k+k'}\mathcal{Q}. \tag{24}$$

As above, one can conclude that the terms which give the main contribution to the drag current are those where $\left|\tilde{\varepsilon}^{(1)}_n(0) - \tilde{\varepsilon}^{(2)}_{n'}(0)\right|$ is smaller than or of the order of $k_{\mathrm{B}}T$ or eV. We will assume that there is only one such difference (otherwise we would have got a sum of several terms of the same structure).

As $\mathcal{Q}$ is a sharp function of k and k', one can take out of the integral all the slowly varying functions and get (the result is given for the general case where $\mu^{(1)} \neq \mu^{(2)}$)

$$I_{\mathrm{D}} = I_0\frac{1}{2}\sinh\left(\frac{eV}{2k_{\mathrm{B}}T}\right)\frac{\dfrac{eV}{4k_{\mathrm{B}}T} - \dfrac{\tilde{\varepsilon}_{nn'}}{2k_{\mathrm{B}}T}}{\sinh\left(\dfrac{eV}{4k_{\mathrm{B}}T} - \dfrac{\tilde{\varepsilon}_{nn'}}{2k_{\mathrm{B}}T}\right)} \times \frac{\dfrac{eV}{4k_{\mathrm{B}}T} + \dfrac{\tilde{\varepsilon}_{nn'}}{2k_{\mathrm{B}}T}}{\sinh\left(\dfrac{eV}{4k_{\mathrm{B}}T} + \dfrac{\tilde{\varepsilon}_{nn'}}{2k_{\mathrm{B}}T}\right)} \tag{25}$$

where

$$I_0 = -\frac{64e^5m^3L(k_{\mathrm{B}}T)^2}{\kappa^2\pi^2\hbar^4}\mathcal{D}_{nn'}. \tag{26}$$

Here $\tilde{\varepsilon}_{nn'} = \tilde{\varepsilon}^{(1)}_n(0) - \tilde{\varepsilon}^{(2)}_{n'}(0)$.

For $eV \ll k_{\mathrm{B}}T$ equation (25) turns into equation (16). Let us consider the opposite case $eV \gg k_{\mathrm{B}}T$. One gets for the drag current

$$I_{\mathrm{D}} = \mathcal{B}\left[\left(\frac{eV}{2}\right)^2 - (\tilde{\varepsilon}_{nn'})^2\right], \qquad \mathcal{B} = -\frac{16e^5m^3L}{\kappa^2\pi^2\hbar^4}\mathcal{D}_{nn'}. \tag{27}$$

This result is non-vanishing only if $|\tilde{\varepsilon}_{nn'}| < eV/2$.

In this section we have discussed a Fermi liquid theory of the Coulomb drag current in a quantum wire brought about by a current in a nearby parallel quantum wire. A ballistic transport in both quantum wires is assumed. The drag current I_{D} as a function of the wire widths comprises one or several spikes; the position of each spike is determined by a coincidence of a pair of levels of transverse quantization, $\varepsilon_n(0)$ and $\varepsilon_{n'}(0)$ in both wires.

3. Luttinger liquid theory of Coulomb drag

In 1D systems *e–e* interaction gives rise to electronic correlations that are believed to destroy the Fermi liquid. Instead, a different state is generated that is usually described as a Luttinger liquid [19, 32] (for reviews see e.g. [20, 33–35]). It is therefore not surprising that in 1D systems *e–e* interaction affects the drag in a different way than in two- or three-dimensional systems. Indeed, in 1D systems interaction strongly enhances the effect, getting stronger with decreasing temperature. As a result, the positive temperature characteristic of the drag resistance from Fermi liquid theory can become a negative one. For sufficiently long wires the drag resistance becomes exponentially large at low temperatures.

This section reviews in the main part the works [15–17], and is organized as follows: Section 3.1 introduces bosonic variables as the appropriate language for the discussion to follow. In section 3.2 the renormalization group method is employed in order to show in which way the drag becomes enhanced by electron correlations. This consideration will also

clarify some relevant energy and length scales of the problem. Section 3.3 elaborates on the influence of the electron spin on the drag, while section 3.4 deals with non-linearities and asymmetric double wires. Section 3.5, briefly discusses the drag in a system with a finite region of interaction.

3.1. Bosonic variables

For treating interactions it is convenient to describe excitations of the many-electron system in terms of collective coordinates: for example by the displacement $\varphi(x)$ of electrons. They are normalized in such a way that density and current fluctuations are given by $\partial_x\varphi(x) = -\sqrt{\pi}(n(x) - n_0)$ and $\partial_t\varphi(x) = \sqrt{\pi}I(x)/e$. Rewriting the Hamilton of an interacting 1D electron gas in $\varphi(x)$ and its canonical conjugated field $\Pi(x)$ yields the Hamiltonian of an elastic string

$$H = \frac{v}{2}\int \mathrm{d}x\, K\Pi^2 + \frac{1}{K}(\partial_x\varphi)^2. \tag{28}$$

The stiffness or interaction parameter K and the velocity v are determined by the parameters of the electronic system. For non-interacting electrons $K = 1, v = v_\mathrm{F}$, while for a system with repulsive interaction $0 < K < 1$ and $v \approx v_\mathrm{F}/K$. The solutions $\varphi(x,t)$ of the Hamiltonian (28) are 1D waves with wave velocity v. In the limit of strong interactions $K \ll 1$, these solutions correspond to the plasma oscillations of the electron density. Contrary to the underlying fermionic operators, the fields φ and Π obey bosonic commutation relations. The substitution of the former by the latter is therefore known as 'bosonization' [19, 20, 33–35].

Excitations of a double wire can be similarly described by the respective displacement fields $\varphi_1(x)$ and $\varphi_2(x)$ of each wire. Assuming a symmetrical system, the two eigenmodes of the density oscillations (at a given wavenumber q) are the symmetric mode (+), where the density in both wires oscillates in phase, and the anti-symmetric mode (−), where the phases of the density oscillations differ by π. A transformation to the corresponding displacement fields $\phi_\pm = (\varphi_1 \pm \varphi_2)/\sqrt{2}$ decouples the Hamiltonian into a symmetric and an anti-symmetric part,

$$H = H_1 + H_2, \qquad H_\pm = \frac{v_\pm}{2}\int \mathrm{d}x\; K_\pm\Pi^2 + \frac{1}{K_\pm}(\partial_x\phi_\pm)^2.$$

Each part has its own set of parameters. In good approximation

$$K_\pm = \left(1 + \frac{V_0 \pm \bar{V}_0}{\pi v_\mathrm{F}} - \frac{V_{2k_\mathrm{F}}}{\pi v_\mathrm{F}}\right)^{-1/2}, \tag{29}$$

and $v_\pm = v_\mathrm{F}/K_\pm$, where $V_0, \bar{V}_0$ are the Fourier transforms of intra-wire and inter-wire interaction $V(x)$ and $\bar{V}(x)$ for small momentum $q \to 0$. V_{2k_F} is the intra-wire backscattering strength ($\delta q = 2k_\mathrm{F}$) [17]. For the range of applicability of expression (29) see [36, 37], where more precise estimates of the Luttinger liquid parameters are given.

So far inter-wire backscattering of electrons, where a large momentum of order $\delta q = 2k_\mathrm{F}$ is exchanged, has not been taken into account. As pointed out in the previous section, this coupling, however, is essential for the drag and must be incorporated in the description. Fortunately, this can also be done in terms of the displacement field, leading to

$$H_\mathrm{b} = \lambda\frac{E_0^2}{\pi v_\mathrm{F}}\int \mathrm{d}x\, \cos(\sqrt{8\pi}\phi_-). \tag{30}$$

The energy E_0 is of the order of the Fermi energy, and the dimensionless coupling λ is given by

$$\lambda = \frac{\bar{V}_{2k_\mathrm{F}}}{2\pi v_-}. \tag{31}$$

Note that the symmetric and anti-symmetric modes still remain decoupled. There is no corresponding term in the intra-wire interaction. The reason is that the backscattering within a wire appears as the exchange part of the forward scattering ($\delta q \to 0$), and therefore can be absorbed in the parameters $K_\pm$ and $v_\pm$ (cf equation (29)).

The origin of the backscattering Hamiltonian H_b becomes clear in the limit of strong repulsive intra-wire interaction. In this case the electrons of each wire form well-correlated states with charge densities periodic in $2\pi/k_\mathrm{F}$. Accordingly, their local interaction energy is 2π-periodic in the relative displacement $(s_1 - s_2)k_\mathrm{F} = \sqrt{8\pi}\phi_-$. The integral over $\cos\sqrt{8\pi}\phi_-(x)$ with an appropriate prefactor therefore gives, to first order, the corresponding part of the total energy.

3.2. Drag

The backscattering Hamiltonian (30) is of sine-Gordon type, and allows for an intuitive understanding of the drag in the case of large couplings λ. Suppose that the total energy is dominated by H_b, the system minimizes its energy by fixing the field ϕ_- to a value $\sqrt{8\pi}\phi_0 = \pi + 2\pi m$, where m an integer number. Accordingly, the relative displacement of electrons in wires 1 and 2 is constant in time and space. This means that two interlocked charge density waves have been formed, such that a current in one wire is necessarily accompanied by an equally large current in the second wire. In this ideal situation the drag is absolute [15].

What happens to the drag if the situation is not that ideal is the topic of this section. Considerable insight with a minimum of calculation effort will be gained by making use of the concept of renormalization.

Neglecting for a while all interactions except for the inter-wire backscattering, the double-wire system can be viewed as a pair of uncorrelated 1D Fermi liquids. As explained in the previous section, the interwire backscattering coupling then causes a drag resistivity $\rho_\mathrm{D} = R_\mathrm{D}/L$, where L is the length of the drag wire, linear in temperature and proportional to λ^2,

$$\rho_\mathrm{D} \approx \rho_0\lambda^2 T/E_0 \tag{32}$$

(cf equation (16) in the limit $T \gg \Delta\varepsilon_n(0)$). To first order the drag only depends on the direct backward scattering part of the interaction. However, higher order contributions to ρ_D include inter- and also intra-wire forward scattering. In one dimension these higher order contributions are crucial and must be taken into account. The renormalization group theory does the job quite elegantly by successively integrating out high energy degrees of freedom down to an energy scale $E < E_0$. As a result, the original ('bare') couplings K_-, λ become renormalized to E-dependent couplings $K_-(E)$ and $\lambda(E)$. The energy scale at which the renormalization procedure has to be stopped can be given by the temperature, system size or even by the coupling $\lambda(E)$ itself, depending on the circumstances. The net effect of higher order processes on the drag between a pair of weakly coupled wire can be summarized by replacing—for example in equation (32)—the bare coupling λ by a

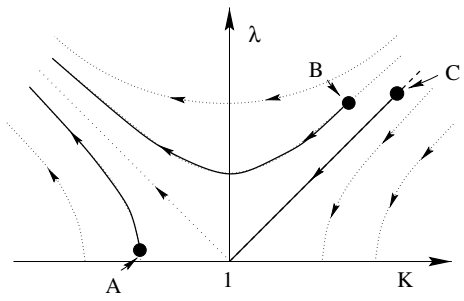

Figure 4. The RG-flow of a double-wire system of spin-less electrons. Point A corresponds to the bare couplings of a double wire with a rather large inter-wire distance $d \gg \lambda_F$, and point B corresponds to wires with narrow spacing $d \ll \lambda_F$. Point C corresponds to a single spin-$\frac{1}{2}$ liquid.

renormalized energy-dependent ('running') coupling constant $\lambda(E)$. Further, good approximations for relevant energy scales can be easily extracted from the renormalization procedure. This should be enough motivation for a short excursion to the renormalization flow of the sine-Gordon model.

3.2.1. Renormalization flow. The flow is well known from a closely related problem, that of an interacting spin-$\frac{1}{2}$ electron liquid [39]. For small couplings $\lambda \ll 1$, it is described by the differential equations

$$\frac{d\lambda}{dt} = (2-2K)\lambda, \qquad \frac{dK}{dt} = -2\lambda^2 K^2, \tag{33}$$

where t denotes the negative logarithm of the rescaled energy, $t = \ln E_0/E$. (The subscript '$-$' is suppressed henceforth.) Figure 4 shows schematically the flow in a K–λ diagram. Each point represents a system characterized by the parameters K and λ. Under renormalization the system develops according to the stream lines in the parameter space. The arrows indicate the direction of decreasing energy scale.

The main feature of the flow is the so-called Kosterlitz–Thouless transition: systems with parameter below the line $K = 1+\lambda$ renormalize towards weaker backward scattering λ, systems above or on the left of this line renormalize towards larger λ. Systems on the right of the transition line flow to the point at $K = 1$ and $\lambda = 0$, which represents a non-interacting Fermi liquid.

Whether a system develops to weaker or stronger couplings λ obviously depends on the location of the bare coupling (subscript '0'), the initial points of the renormalization trajectories. For systems with symmetrical interaction, $V(x) = \bar{V}(x)$, as is the case for a spin-$\frac{1}{2}$ electron liquid, one finds for small V_{2k_F} that $K_0 = 1 + \lambda_0$, i.e. the initial point lies exactly on the transition line. These systems (marginally) renormalize towards the non-interacting Fermi point. This is indeed the expected behaviour for the spin-mode of an electron liquid. (The spin-mode corresponds to the anti-symmetric mode $(-)$.) If one could measure the relative drag of spin-up and spin-down electrons, one would find that due to the additional temperature dependence in $\lambda(T)$, the drag resistivity decays with temperature even faster than the naively expected linear behaviour.

Interestingly, the situation is completely different for a real double-wire system. Due to the spatial separation of the two wires, the intra-wire interaction $V(x)$ always exceeds the inter-wire interaction $\bar{V}(x)$. Inspection of equations (29) and (31) reveals that as a consequence the initial point is always above or on the left of the transition line, where λ renormalizes to higher values. Therefore, here the backscattering coupling λ, although usually much smaller than that in the previous case, increases with decreasing energy scale or temperature. Hence, for low temperatures (and long wires, see below) the drag resistivity will always be larger than that predicted by the Fermi theory. This will be described more quantitatively in the next paragraph.

3.2.2. Temperature dependence of the drag. Before rushing into a discussion of the various kinds of regimes with different types of temperature dependencies, it is advisable to clarify the relevant energy and length scales. There is $E_0 \sim E_F$, the largest energy scale, the temperature T_L, at which the thermal wavelength becomes of the order of the system size and the actual temperature T. The corresponding length scales are the Fermi wavelength $\lambda_F \sim E_0/v$, the system size L and the thermal wavelength $L_T = v/T$. Less obviously, a fourth energy and length scale are given by the sine-Gordon Hamiltonian $H_- + H_b$: the energy (mass) M of a soliton and its width L_s. The soliton mass M coincides with the energy scale at which the renormalization procedure breaks down, the soliton width L_s is the corresponding length scale. The relative order of these scales classify several different regimes.

For high temperatures $T > T_L, M$ the renormalization of λ is terminated by T. Thus, $\lambda = \lambda(T)$. In this case the temperature dependence of $\lambda(T)$ can be approximately determined by integrating the flow equations (33), leading to a

$$\lambda(T) = \lambda_0 \left(\frac{T}{E_0}\right)^{2K-2}. \tag{34}$$

This result inserted in equation (32) gives the temperature dependence,

$$\rho_D \approx \rho_0 \lambda_0^2 \left(\frac{T}{E_0}\right)^{4K-3}, \tag{35}$$

valid for $T_L, M \ll T \ll E_0$. The e–e interaction changes via the renormalization of the backscattering coupling, the linear temperature dependence known from the 1D Fermi liquid to a temperature scaling with an interaction-dependent power $\chi = 4K-3$. For sufficiently strong interaction, K can assume values below 3/4. Then the power χ becomes negative and the drag increases with decreasing temperature. For vanishing interaction, $K = 1$, equation (35) goes over to the linear behaviour of the Fermi liquid.

Lowering the temperature below M or T_L, two scenarios are possible: if the wire is sufficiently long, $L \gg W$, at a temperature $T \sim M$ the system eventually enters the strongly coupled regime, where $\lambda(T) \sim 1$. For short wires, $L \lesssim L_s$, this regime can not be reached. Here the renormalization halts at a temperature $T \sim T_L$, where the thermal wavelength is of the order of the system size. In this case even at low temperatures the systems are weakly coupled, $\lambda(T_L) \ll 1$.

In the strongly coupled regime the energy is dominated by the backscattering term H_b, giving rise to an almost absolute drag. Deviations from this ideal drag correspond to processes

where the relative displacement $\sqrt{8\pi}\phi_-$ slips from one global minimum position, say at π, to a neighbouring one at $-\pi$ or 3π. At temperatures $T < M$ these processes are enabled by thermally activated solitons moving along the wire. As a result the drag resistivity shows for $T < M$ an activated behaviour,

$$\rho_{\mathrm{D}}(T) \sim \tilde{\rho}_0 \, \mathrm{e}^{M/T}.$$

This behaviour changes again when the temperature falls below T_{L} (for the strong coupling regime considered, $T_{\mathrm{L}} < M$). It has been shown [16] that the drag then decreases linearly with temperature, due to the on set of coherent soliton-tunnelling. At even lower temperatures $T < \sqrt{T_{\mathrm{L}} M}\exp(-M/T_{\mathrm{L}})$ the drag decreases with T^2 [16].

In the weakly coupled regime, the drag resistance decays $\propto T^2$ as the temperature drops below T_{L}. This can be understood as follows: having renormalized down to an energy T_{L}, the original Fermi wavelength $\lambda_{\mathrm{F}} \sim v/E_0$ has become enlarged to a rescaled wavelength $\lambda_{\mathrm{F}}(T_{\mathrm{L}}) \sim v/T_{\mathrm{L}} = L$. Hence, the wires of length L have effectively shrunk down to point-like constrictions connecting electronic reservoirs on either side. The drag in this situation is equivalent to that in a pair of 1D Fermi liquids ($K = 1$) that interact over a short length $\lesssim L_{\mathrm{T}}$ only. As will become clear in section 3.5, the drag is then proportional to T^2 (cf section 3.5, $K = 1$).

The temperature scale T_* at which the system enters the strongly coupled regime is given by the soliton mass $T_* = M$. Estimating it by $\lambda(T_*) \sim 1$ with the approximate expression (34) yields

$$T_* \sim E_0 \, \lambda^{\frac{1}{2-2K}}. \tag{36}$$

The minimum wire length required is then $L_* = v/T_* = \lambda_{\mathrm{F}} \lambda^{-\frac{1}{2-2K}}$.

3.3. Electron spin

For comparison with experiments, the treatment of the electron spin is mandatory. To this end one can introduce bosonic fields $\varphi_{c/s}$ that are related to the charge/spin density $n_c = n_\uparrow \pm n_\downarrow$ in the same way as φ is related to the density n of spinless particles above. For a double wire, this results in a total of four modes: symmetric and anti-symmetric charge modes ($c+$ and $c-$) as before, and, additionally, symmetric and anti-symmetric spin modes ($s+$ and $s-$). Each mode is again described by a quadratic Hamiltonian of the type (28) with corresponding interaction parameters $K_{c\pm}$, $K_{s\pm}$, etc.

The neutral spin-modes are not affected by the interaction, wherefore $K_{s\pm} = 1$ and $v_{s\pm} = v_{\mathrm{F}}$. Nevertheless, despite their neutrality, the spin-modes weakly couple to the anti-symmetric charge mode $c-$ via backscattering processes. Hence, the drag is influenced by the spin degree of freedom [17].

A quantitative analysis of the weakly coupled regime can be done again by making use of renormalization along the lines described above. The main results are summarized below: in the presence of spin the inter-wire backscattering coupling scales towards stronger couplings. However, fluctuations in the neutral spin-modes moderate the enhancement due to the interactions. This is reflected by an effective interaction parameter

$$K_{\mathrm{eff}} = \frac{K_{c-} + K_{s\pm}}{2} = \frac{K_{c-} + 1}{2}$$

which is closer to the non-interacting value 1 than the original K_{c-}. The parameter K_{c-} is given by

$$K_{c-} \approx \left(1 + 2\frac{V_0 - \bar{V}_0}{\pi v_{\mathrm{F}}} - \frac{V_{2k_{\mathrm{F}}}}{\pi v_{\mathrm{F}}}\right)^{-1/2}. \tag{37}$$

As a result, in the weakly coupled regime the drag resistance scales with temperature as

$$\rho_{\mathrm{D}} \approx \rho_0 \lambda_0^2 \left(\frac{T}{E_0}\right)^{2K_{c-}-1}$$

(cf equation (35)). The cross-over temperature T_* turns out to be approximately

$$T_* \sim E_0 \, \lambda^{\frac{1}{1-K_{c-}}}.$$

Comparison with equation (36) again reveals the moderating effect of the spin. If two systems have similar interaction constants $K_- \approx K_{c-}$, but one is spin polarized while the other is not, their respective cross-over temperatures and lengths are related by

$$\left(\frac{T_*}{E_0}\right)^2_{\mathrm{pol}} \approx \left(\frac{T_*}{E_0}\right)_{\mathrm{unpol}}, \qquad \left(\frac{\lambda_{\mathrm{F}}}{L_*}\right)^2_{\mathrm{pol}} \approx \left(\frac{\lambda_{\mathrm{F}}}{L_*}\right)_{\mathrm{unpol}}.$$

Since $T_*/E_0 \sim \lambda_{\mathrm{F}}/L_*$ is usually a small number, the cross-over temperature of the spin-unpolarized system is smaller than that of a comparable spin-polarized system by orders of magnitudes .

3.4. Non-linear drag and mismatching Fermi momenta

So far our considerations were confined to the linear regime ($I \to 0$) of a symmetrical double-wire system. This section extends the discussion to both the non-linear regime, and systems with a misfit in the Fermi momenta, $\delta k = k_{\mathrm{F1}} - k_{\mathrm{F2}} \neq 0$.

It is again useful to look first at the associated energies. A finite current I in the active wire defines an energy $\Omega = I/e$, and the energy associated to the misfit is of course $\Delta = v\delta k$. Non-linearities of the drag voltage V_{D} in the current I, or an effect of the misfit δk, will be significant only if the corresponding energies $|\Omega|$ or $|\Delta|$ exceed T, T_{L} and M.

In the weakly coupled regime both cases can be analysed by perturbative methods. Finite currents and a non-vanishing δk can be treated by a transformation $\phi(x,t) \to \phi(x,t) + \Delta x/v + \Omega t$. The term linear in x describes the density difference ($\partial_x\phi \propto (n_1 - n_2)$) and the term linear in t corresponds to a Galilei boost of the active wire. Accordingly, H_{b} becomes

$$H_{\mathrm{b}} = \lambda \frac{E_0^2}{\pi v_{\mathrm{F}}} \int \mathrm{d}x \, \cos\sqrt{8\pi}(\phi + \Delta x/v + \Omega t).$$

It is possible to derive a closed expression for the drag voltage V_{D} as a response to this perturbation [38]. It is valid for arbitrary ratios Ω/Δ, and can be written as

$$\frac{eV_{\mathrm{D}}}{L} = C\frac{E_0^2\lambda_0^2}{v}\left(\frac{T}{E_0}\right)^{4K} \{A(\Omega-\Delta)B(\Omega+\Delta) + A(\Omega+\Delta)B(\Omega-\Delta)\}. \tag{38}$$

C is a numerical constant of order unity, and A and B are temperature-dependent functions, given by

$$A(E) = \int \mathrm{d}s \, \mathrm{i} \sin\left(\frac{E}{E_0}s\right)\left(\pi\left(\frac{1}{s} + \mathrm{i}\right)\sinh\frac{Ts}{\pi E_0}\right)^{-2K},$$

and a similar expression with cos instead of i sin for B. This expression holds also for vanishing Δ, Ω, where it leads to the result (35). For current and δk large compared to temperature, $\Omega, \Delta \gg T$, equation (38) reduces to [15]

$$\frac{eV_D}{L} = \text{const}\ \lambda_0^2 (\Omega^2 - \Delta^2)^{2K-1}, \qquad \text{for } |\Delta| < |\Omega|$$
$$= 0 \qquad \text{otherwise.}$$

For non-vanishing Δ the drag vanishes as long as the current is below a threshold value. For larger currents the voltage shows a power-law dependence on the current. A thorough discussion of the non-linear I–V characteristic can be found in [15].

Actually, at finite temperatures the drag does not vanish completely for $|\Delta| > |\Omega|$, rather it shows an activated behaviour as in the case of 1D Fermi liquids. This can be made more explicit [38]. Evaluating expression (38) in the limit $\Omega \to 0$ at finite Δ results in a drag resistivity

$$\rho_{\Delta,T} = \rho_0 \lambda^2 \left(\frac{T}{E_0}\right)^{4K-3} F_{2K}(\Delta/T), \tag{39}$$

where F_{2K} is an interaction-dependent function defined by

$$F_{2K}(\varepsilon) = N_{2K}(\varepsilon)\frac{dN_{2K}}{d\varepsilon}(-\varepsilon) + N_{2K}(-\varepsilon)\frac{dN_{2K}}{d\varepsilon}(\varepsilon),$$
$$N_{2K}(\varepsilon) = \lim_{\delta\to 0}\int ds\, e^{is\varepsilon/\pi}\left(\left(\frac{\delta}{s} + i\right)\sinh s\right)^{-2K}.$$

F_{2K} is a continuous function. It decays exponentially at large positive arguments, $F_{2K}(\varepsilon) \sim \exp -\varepsilon$, and behaves algebraically for large negative arguments, $F_{2K}(\varepsilon) \sim |\varepsilon|^{K-1}$. The result obtained for non-interacting 1D Fermi liquids is recovered by putting $K = 1$. In this case

$$N_2(\varepsilon) = \frac{1}{\pi}\frac{\varepsilon}{e^{\varepsilon} - 1},$$

such that the expression (39) corresponds to equation (16). While $N_2(\varepsilon)$ bears some resemblance to the Bose distribution, for the special interaction parameter $K = 1/2$ one obtains exactly the Fermi function

$$N_1(\varepsilon) = \frac{1}{e^{\varepsilon} + 1}.$$

For general parameter K, an analytical expression for N_{2K} is lacking. It is an open question whether the functions N_{2K} are related to the exclusion statistics of fractional excitations in the Luttinger liquids.

3.5. Finite interaction region

Double wires that interact only over a region of finite length $l < L$ have also been investigated [12, 13]. For temperatures $T < v/l$, this problem can be mapped to the classical problem of a Luttinger liquid with a single impurity. Qualitatively, these systems behave similar to those considered in the previous sections. In the weakly coupled regime, the drag scales with temperature with an interaction-dependent exponent, $4K - 2$. A strongly coupled regime with almost absolute drag at zero temperature exists as well. However, it is reached only for sufficiently strong interaction $K < 1/2$. For $K > 1/2$ the inter-wire backscattering coupling renormalizes to weaker couplings, such that the drag vanishes for $T \to 0$.

4. Experimental search for 1D Coulomb drag

Although a fair amount of theoretical work has been available on Coulomb drag between 1D electron systems, there has been a conspicuous absence of experimental work. This may be attributed to two difficulties encountered in measuring the 1D drag. First, since it is a very small effect, the drag voltage usually has a very small magnitude and must be clearly distinguished from spurious signals. Second, and perhaps the major difficulty, has been the difficulty in creating parallel, electrically isolated, quantum wires with a spatial separation large enough to completely suppress inter-wire, while small enough to give a drag voltage of a reasonable magnitude. It was only recently that Debray *et al* [5] reported the first experimental observation of Coulomb drag between ballistic quantum wires. The same authors later published a more comprehensive experimental work [6] on the subject. Work along the same lines has lately been reported by Yamamoto *et al* [7]. In the following, we give a brief outline of the reported experimental work and an analytical discussion of the results in the framework of the Fermi and the Luttinger liquid theory as discussed in section 2 and 3.

4.1. Experimental techniques for dual-wire sample realization

The samples used for 1D Coulomb drag measurements consisted of two electrically isolated, parallel quantum wires, with a small spatial separation. Such samples were fabricated from AlGaAs/GaAs heterostructures with a high-mobility ($\cong 10^6$ cm^2/Vs) two-dimensional electron gas (2DEG) at the interface. The dual-wire samples were fabricated using high-resolution electron beam lithography, combined with deep chemical etching. The samples used so far were made in a planar geometry by depletion of a single 2DEG layer by three surface Schottky gates [5–7] deposited on the heterostructure wafer. Figure 5 gives a schematic top view of the planar device and the scanning electron micrograph of a typical device [6]. U, M and L are surface Schottky gates.

Dual-wire samples for drag measurements can also be made in a vertical geometry [4] from two vertically stacked quantum well (QW) structures with a 2DEG in each well (such samples have not yet been used). The advantage of the planar geometry is that the inter-wire separation can be changed *in situ* by changing the bias voltage of the central gate M. The disadvantage is that the narrow central gate creates a soft lateral potential barrier, and to prevent tunnelling between the wires the width of this barrier has to be of sufficient magnitude, which sets a limit to the minimum inter-wire distance that can be used without electron tunnelling interfering. Samples with a vertical geometry have been widely used for studying Coulomb drag between 2D electron layers [2]. The main advantage of the vertical geometry is that very small inter-wire separation (the barrier width) can be obtained without tunnelling between wires. Since the magnitude of the drag is expected to decrease exponentially with inter-wire separation, one can expect to observe enhanced drag with the vertical samples because of the smaller separation that can be achieved with such samples. The major disadvantage is that the inter-wire separation cannot be changed *in situ*, in contrast to the

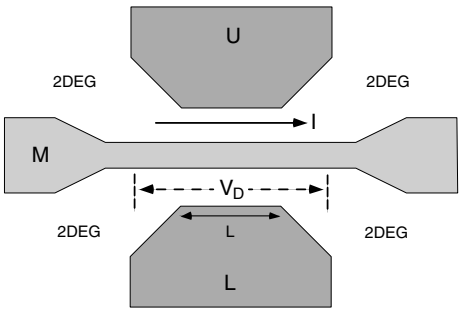

(*a*)

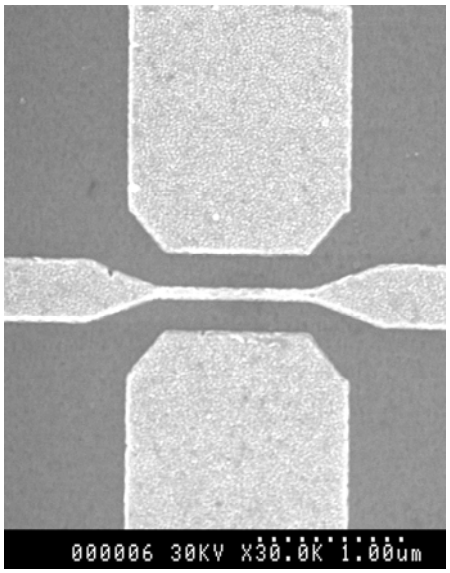

(*b*)

Figure 5. (*a*) Schematic top view of a planar Coulomb drag device. U, M and L are surface Schottky gates. (*b*) A scanning electron micrograph of a typical device with middle gate width of 50 nm.

planar case. Also, it is not obvious whether the widths of the two wires can be independently changed through the use of the mutually aligned top and bottom split gates.

4.2. Experimental observation of Coulomb drag

In their work, Debray *et al* [6] used a planar geometry of quantum wires, as shown in figure 5, of lithographic length $L = 2\,\mu$m with a middle gate M of lithographic width 50 nm. The drag voltage V_D was measured with a drive voltage V_{DS} in the linear regime of ballistic electron transport as a function of the width of the drive wire by adjusting the bias voltage V_U, while the width of the drag wire was adjusted to have the Fermi level E_F just above the bottom of its lowest 1D subband. An appropriate negative bias voltage V_M was applied to the middle gate to ensure total absence of inter-wire tunnelling. Measurements were done in the *absence* of any such tunnelling. Figure 6(*a*) shows the measured drag voltage V_D as a function of the width of the drive wire. The drag voltage is found to show peaks, which occur in the rising parts between the plateaus of the drive wire conductance. This suggests that they occur when the 1D subbands of the wires are aligned and the Fermi wave vector k_F is small. Measurements carried out in a magnetic field $B = 0.86$ T perpendicular to

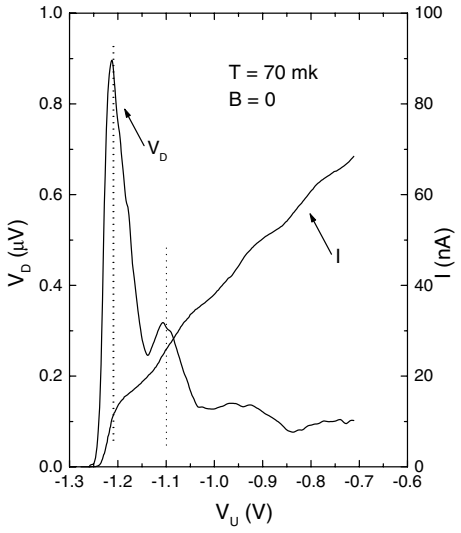

(*a*)

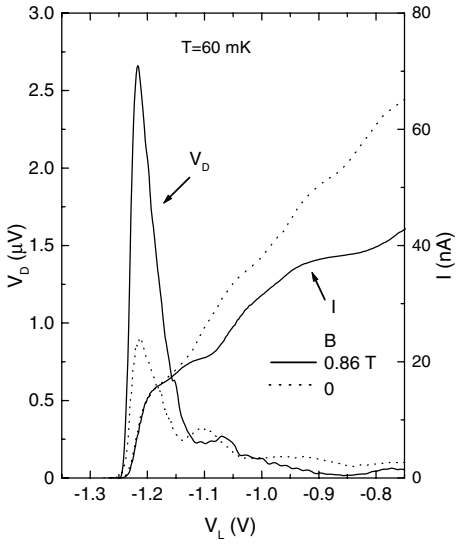

(*b*)

Figure 6. The drag voltage V_D and drive current I as a function of drive wire width at a drive voltage $V_{DS} = 300\,\mu$V [6]: (*a*) in zero magnetic field with the upper wire as the drive wire and (*b*) in a magnetic field of 0.86 T with the bottom wire as the drive wire.

the plane of the device shown in figure 6(*b*) indicate identical behaviour except that the magnitude of V_D is enhanced almost by a factor of 3.

In order to have unambiguous evidence that the observed drag voltage V_D is indeed due to the Coulomb drag effect, the authors measured the dependence of V_D and R_D on the inter-wire separation and the temperature. Figure 7 shows the dependence of V_{DM}, the height of the first V_D peak of figure 6(*b*) and the corresponding R_D as a function of the middle gate bias voltage V_M. The two quantum wires (figure 5) were spatially separated by an effective distance d due to the depletion by V_M of the 2DEG under the middle gate M. In the voltage range of interest, d was experimentally found to vary almost linearly with V_M according to

$$d = d_0 + \alpha\,(V_0 - V_M)\,, \tag{40}$$

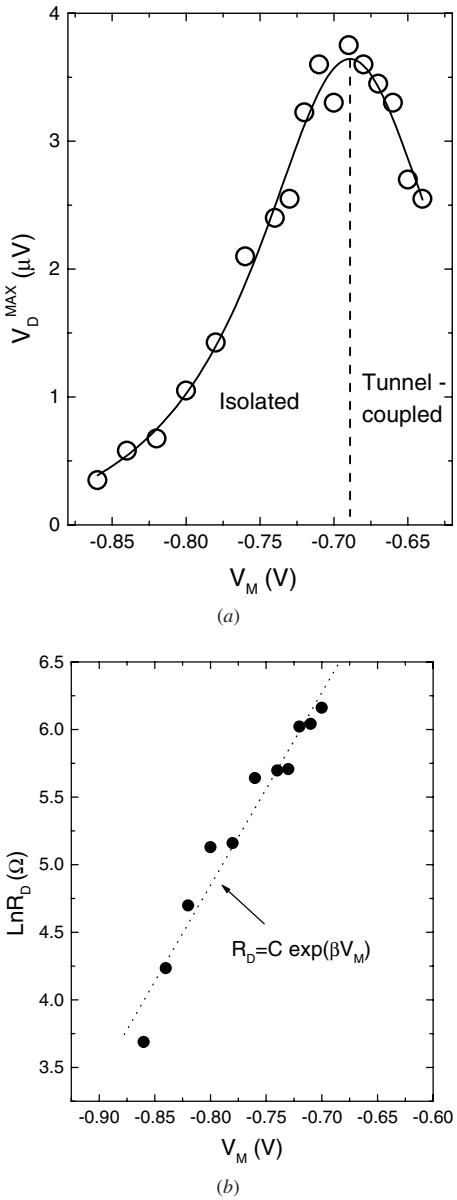

Figure 7. Dependence of the drag response on inter-wire separation d via the middle gate voltage V_M [6]. (*a*) The maximum V_{DM} of the first drag peak of figure 6(*b*) as a function of V_M. (*b*) The natural logarithm of the corresponding drag resistance R_D as a function of V_M. The dotted line is a linear fit to the data points.

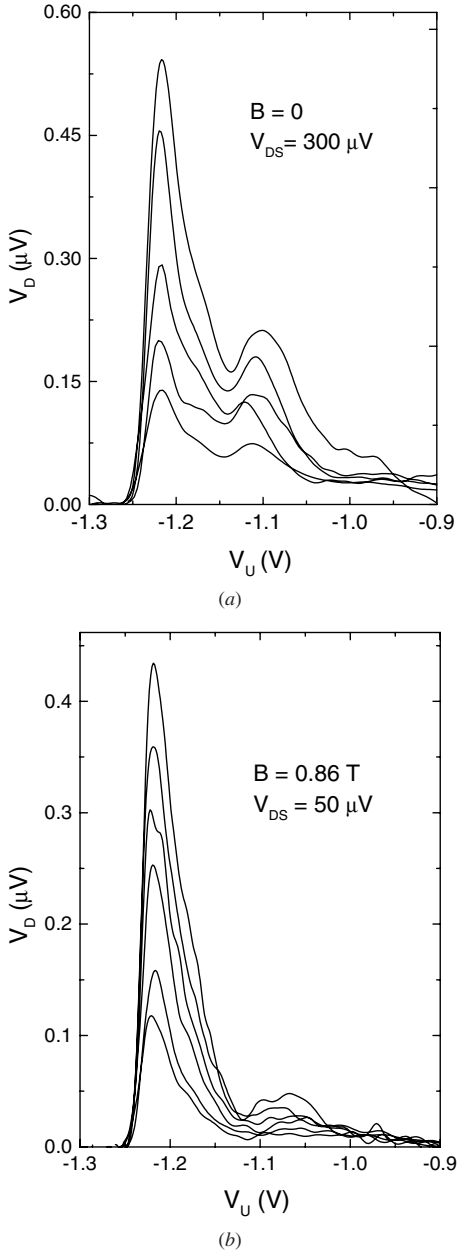

Figure 8. The dependence of drag voltage on temperature [6]. (*a*) The drag voltage V_D as a function of the width of the upper (drive) wire in zero magnetic field with $V_{DS} = 300\ \mu$V at 70, 180, 300, 450 and 900 mK, corresponding to curves in order of decreasing peak height. (*b*) The same as in (*a*) but in a magnetic field of 0.86 T with $V_{DS} = 5\ \mu$V at 60, 180, 300, 450, 900 mK and 1.2 K.

where V_0 is the value of V_M for which the 2DEG under M is just depleted and α gives the total spatial displacement of the two depletion edges of M with respect to its bias voltage. d_0 is a constant for the same device and is nominally equal to the lithographic width of the gate M. One can change d by varying V_M. In equation (40), V_0 and α were determined experimentally. The dependence of R_D on V_M was found to be exponential and can be described well by the relation, $R_D \propto e^{\beta V_M}$, where $\beta \cong 14.2(9)\ V^{-1}$.

The temperature dependence of Coulomb drag is a crucial feature that can be used to probe which of the two theoretical models, the FL or the LL theory, constitutes a more appropriate description of 1D Coulomb drag. Measurements, as shown in figure 6, carried out in the temperature range 60 mK to 1.2 K are shown in figure 8. A decrease of V_D with increasing temperature was observed. The dependence of the drag resistance R_D on temperature corresponding to V_{DM} is shown in figure 9 for both, in the absence and in the presence of an applied magnetic field B. The temperature dependence can be described well by the power law, $R_D \propto T^x$, with $x = -0.77(2)$ and $-0.73(6)$ for $B = 0$ and $B = 0.86$ T, respectively. It is interesting to note that the data points at temperatures lower than 180 mK, for zero field, and 300 mK, for non-zero field, fall below the power-law curve, indicating a suppression of the drag effect.

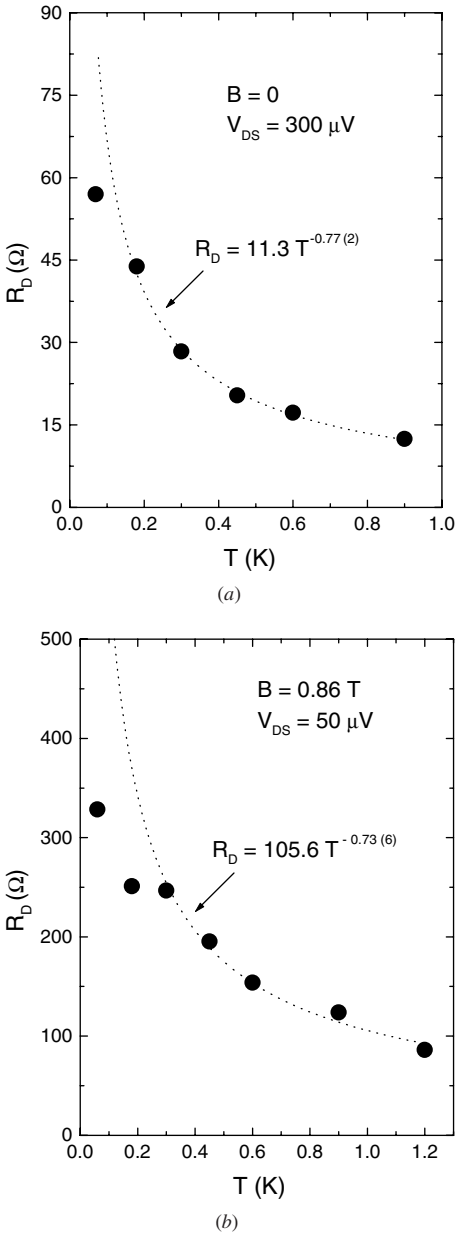

Figure 9. The temperature dependence of drag resistance R_D corresponding to V_{DM} of the first drag peak of figure 8 in zero field (*a*) and in a field of 0.86 T (*b*) [6]. Note that the data points at the low end of the temperature range fall below the power-law curve.

Lately, using a lateral sample geometry, very similar to that shown in figure 5(*a*), Yamamoto *et al* [7] have reported the observation of Coulomb drag and the influence of an applied magnetic field on it. Their results corroborate those of Debray *et al* [5, 6]. In their work, Yamamoto *et al* also reported the observation of a negative drag. However, since the negative drag was observed only when the drive wire was completely pinched off, it is highly questionable if the effect observed is due to Coulomb drag.

4.3. Discussion

The origin of the observed peaks in the drag voltage V_D (figure 6) can be understood when one considers equations (16)–(21). Since V_D is directly proportional to the drag current I_D, V_D will show maxima whenever any two 1D subband bottoms of the two wires line up and the Fermi wave vectors in the two wires are equal and small. As seen from figure 6, the occurrences of the drag peaks correspond to these conditions. The first peak in V_D occurs when the Fermi level is just above the bottoms of the lowest 1D subbands of both wires. Similarly, the second peak occurs when the lowest subband of the drag wire lines up with the second subband of the drive wire. Both the increase and the narrowing of the first drag peak in a magnetic field of 0.86 T (figure 6(*b*)) can be attributed to an increase of the density of states in 1D subbands due to the magnetic-field-induced enhancement of the electron effective mass. The reduction in the magnitude of the drag peak as we move away from the first peak towards higher values of V_U can be attributed to an increase in the effective inter-wire separation of the wires. This dependence is explained in detail later. Since we are mainly concerned with 1D transport in the fundamental mode, we restrict our discussion here to the region of the first drag peak.

To understand the dependence of drag on the inter-wire distance shown in figure 7, we note that the matrix element of the backscattering probability depends on the inter-wire distance d via the modified Bessel function $K_0(2k_Fd)$ (section 2, equation (11)), which is an exponential function of its argument for $2k_Fd \gg 1$. The same dependence also results from the LL theory [28]. Under this condition, an exponential decrease of R_D with d is expected according to $R_D \propto \exp(-4k_Fd)$. This is consistent with the results of figure 7. Using the experimentally determined values $\beta = 14.2\,V^{-1}$ and $V_0 = -0.4\,V, \alpha = 580\ nm\,V^{-1}$, we find $k_F = 6.1 \times 10^6\ m^{-1}$. Surprisingly, this corresponds to a low density of about 8 electrons per 2 μm wire segment and a mean electron distance $\bar{r} \approx 250\,nm$ in the wire. When V_M is in the range of -0.7 to -0.8 V, we have (equation (40) $d \cong 0.2\,\mu m$. This gives $2k_Fd \cong 3$, so the approximation of $2k_Fd \gg 1$ is reasonable. This exponential decrease of R_D with d also explains why the height of the drag voltage peaks in figure 6 decreases so rapidly as V_U increases. An increase in V_U increases the width of the drive wire and hence d. The decrease of R_D for $V_M > -0.7\,V$ occurs due to tunnelling of a considerable fraction of the current from the drive wire to the drag one, reducing the measured R_D.

The experimental observed features of the drag effect discussed above, namely, the origin of the drag voltage peaks, the effect the magnetic field and the inter-wire separation dependence, can all be understood in the framework of both the FL and the LL theory. It is the temperature dependence of the drag that is the crucial feature—it can be used to determine which of the two theoretical models constitutes a more appropriate description of 1D Coulomb drag observed under the given experimental conditions. The observed temperature dependence of R_D, shown in figure 9, is in sharp contrast with the linear temperature dependence predicted by the FL theory (equation (19)). The unusual temperature dependence cannot be attributed to a temperature-induced modification of the wire conductance, since the latter is found to be almost unchanged over the temperature range of the measurements. A reduction of the inter-wire Coulomb coupling due to enhanced screening by the reservoirs and gates is very unlikely at such small temperatures. On the other hand, it is conceivable that

a correlated LL behaviour is established in the wires. Indeed, it is hardly surprising that the temperature dependence of R_D does not fit into a FL scenario, because for the experimental condition of the first drag peak the ratio r_s of $\bar{r}$ and the Bohr radius a_B, $r_s = \bar{r}/a_B \approx 26$ is large.

The smallness of the drag resistance ($R_D < 100\,\Omega$) in zero magnetic field indicates a weak inter-wire back scattering coupling. In this case, according to the LL model R_D should obey a power law as long as the thermal length L_T is well between the wire length $L = 2\ \mu$m and the mean electron distance $\bar{r} \approx 250$ nm in the wire. For spin-unpolarized electrons, valid for the data shown in figure 9, the LL description predicts a power-law temperature dependence of R_D with exponent $x = 2K_{c-} - 1$ (equation (38)). The data shown in figure 9 indeed show a power-law dependence of R_D on temperature with $K_{c1} = 0.12$. Let us see if the condition $\bar{r} < L_T < L$ is fulfilled in the experiment. Given a Fermi wavevector of $k_F \approx 6\,\mu\text{m}^{-1}$ we find that $L_T = h v_F/K_{c-}k_B T$ is equal to the wire length $L = 2\ \mu$m at a temperature $T_L \cong 250$ mK, and that L_T approaches $\bar{r} \approx 250$ nm at a temperature of about 2 K. Here v_F/K_{c-} is the group velocity of the relative electron-density fluctuations and $h/k_B T$ is the quantum lifetime associated with the thermal energy $k_B T$. This means that there is a narrow temperature range window in which a power-law temperature dependence of R_D might be expected, and it is observed experimentally. At temperatures below T_L, when $L < L_T$, the electron coming from the lead to the wire does not have time to accommodate itself in the LL. This should result in a weaker drag than the power-law dependence. The experimental data of figure 9 are consistent with this analysis. At lower temperatures we do indeed observe a tendency to a weakening of the drag with respect to the power-law dependence.

The negative power-law temperature dependence is not the only experimental feature that cannot be understood in terms of the FL theory of Coulomb drag. The experimental value of R_D (figure 9(a)) at $T = 60$ mK is more than an order of magnitude larger than that given by the FL theory (equation (19)). That the measured drag is larger could be explained by the interaction-normalized inter-wire backscattering probability, which should be larger than the bare one (equation (34)).

Comparison of figures 9(a) and (b) shows that the influence of the magnetic field on the temperature dependence is not significant. This may signify that Zeeman spin splitting at $B \leqslant 1$ T is not important yet, otherwise the exponent x should change (equation (35)). Indeed, a clear signature of spin splitting in the measured conductance staircase was not observed at this field. The magnetic field, however, increases v_F for the same position of the Fermi level. This makes L_T larger at the same temperature compared to that in zero field. This can explain why in a magnetic field a deviation from the power-law dependence occurs at a higher temperature (figure 9(b)).

We have interpreted above the experimental data in terms of Coulomb drag only. Considering the large inter-wire separation for which the drag measurements were made, one cannot rule out the possibility of an acoustic phonon-mediated drag (PMD) contribution to the measured drag resistance. Recent theoretical work [40, 41] on 1D PMD based on Fermi liquid description predicts that PMD is negligible compared to Coulomb drag for $2k_F d < 5$. Also, for a dual-wire sample shown in figure 5, R_D should increase exponentially with temperature in the range 100–600 mK and does not decrease exponentially with inter-wire separation d. The data shown in figures 7 and 9 qualitatively contradict these predictions. This allows us to conclude that the PMD contribution, if present at all, is insignificant.

5. Future prospects

It is quite obvious from the content of section 4 that substantial experimental work remains to be done to gain a comprehensive understanding of the physics of Coulomb drag between interacting 1D electron systems and to explore the conditions under which such systems behave as a Fermi liquid or a Luttinger liquid. Since the measurement of the Coulomb drag also provides a new experimental tool to probe the LL state that cannot be done from the measurement of the conductance alone, extensive experimental work on the subject is needed to put the LL model of interacting 1D systems on a firm footing. Though the theory of Coulomb drag has considerably outstripped experimental work, many open questions need to be addressed in the theoretical area as well.

On the experimental side, work should be focused on measurements that can distinguish between a LL and a FL state and can provide information about the existence and the nature of the LL state. This is an extremely important area for condensed matter physics. The few papers published so far, claiming to have observed a Luttinger liquid, have not been convincing. In this respect, it would be highly interesting to study the drag between spin-polarized systems, since the LL theory predicts different exponents for spin-polarized and unpolarized cases and manifestation of the spin effect should be quite different in the Fermi liquid and the Luttinger liquid state. Another interesting experimental possibility is to study drag when the wire length L falls below the thermal length L_T to investigate if the drag resistance R_D decays $\propto T^2$ as predicted by LL theory. When the number of electrons in the wires is very small (section 4), one should expect relatively large fluctuations of the drag current or voltage, such as shot noise [42, 43], and possible reversal of the sign of drag leading to negative drag [44]. Observation of this noise can also provide valuable information on correlated electron state. One could also envision a search for 1D spin Coulomb drag [45]. Finally, it is also important to study acoustic phonon-mediated drag (PMD) [40, 41] since under certain conditions it can be comparable to and even larger than the Coulomb drag. If such a PMD is present in the experimental measurements, one has to find ways to separate it from the Coulomb drag.

The theory of Coulomb drag based on the LL model is far from mature and many open questions need to be addressed such as the effect of disorder, the influence of tunnelling between the wires, etc. Although the power-law temperature dependence of the drag resistance is a signature of the Luttinger liquid state, a careful analysis of various limiting cases based on the Fermi liquid approach should be carried out to make sure that under no circumstances can it give a similar temperature dependence. It is equally important to investigate the physical situations and interactions (within the wires and with the

reservoirs) that favour transition of the Fermi liquid into the Luttinger liquid and vice versa.

Acknowledgment

The authors wish to thank H L Hartnagel for his encouragement and interest in this work.

References

[1] Pogrebinskii M B 1977 *Sov. Phys.–Semicond.* **11** 372
[2] For a recent review see Rojo A 1999 *J. Phys.: Condens. Matter* **11** R31
[3] Nozieres P 1997 *Theory of Interacting Fermi Systems* (Reading, MA: Addison-Wesley)
[4] Moon J S, Blount M A, Simmons J, Wendt J R, Lyo S K and Reno J L 1999 *Phys. Rev.* B **60** 11530
[5] Debray P, Vasilopoulos P, Raichev O, Perrin R, Rahman M and Mitchel W C 2000 *Physica* E **6** 694
[6] Debray P, Zverev V, Raichev O, Klesse R, Vasilopoulos P and Newrock R S 2001 *J. Phys.: Condens. Matter* **13** 3389
[7] Yamamoto M, Stopa M, Tokura Y, Hira yama Y and Tarucha S 2001 *Proc. 25th Int. Conf. on the Physics of Semiconductors* (Singapore: World Scientific)
[8] Gurevich V L, Pevzner V B and Fenton E W 1998 *J. Phys.: Condens. Matter* **10** 2551
[9] Sirenko Y M and Vasilopoulos P 1992 *Phys. Rev.* B **46** 1611
[10] Hu Ben Yu-Kuang and Flensberg Karsten 1996 *Hot Carriers in Semiconductors* ed K Hess *et al* (New York: Plenum)
[11] Tanatar B 1998 *Phys. Rev.* **58** 1154
[12] Komnik A and Egger R 1998 *Phys. Rev. Lett.* **80** 2881
[13] Flensberg K 1998 *Phys. Rev. Lett.* **81** 184
[14] Raichev O and Vasilopoulos P 2000 *Phys. Rev.* B **61** 7511
[15] Nazarov Y V and Averin D V 1998 *Phys. Rev. Lett.* **81** 653
[16] Ponomarenko V V and Averin D V 2000 *Phys. Rev. Lett.* **85** 4928
[17] Klesse R and Stern A 2000 *Phys. Rev.* B **62** 16912
[18] Gurevich V L and Muradov M I 2000 *Pis'ma Zh. Eksp. Teor. Fiz.* **71** 164 (Engl. Transl. 2000 JETP *Lett.* **71** 111)
[19] Haldane F D M 1981 *J. Phys.* C **14** 2585
Haldane F D M 1981 *Phys. Rev. Lett.* **47** 1840
[20] Voit J 1994 *Rep. Prog. Phys.* **57** 977
[21] Bockrath M, Cobden D H, Lu J, Rinzler A G, Smalley R E, Balents L and McEuen P L 1999 *Nature* **397** 598
[22] Auslander O M, Yacoby A, de Picciotto R, Baldwin k W, Pfeiffer L N and West k W 2000 *Phys. Rev. Lett.* **84** 1764
[23] Takiainen R, Ahlskog M, Penttila J, Roschier L, Hakonen P, Paalanen M and Sonin E 2001 *Phys. Rev.* B **64** 195412
[24] Auslander O M, Yacoby A, de Picciotto R, Baldwin k W, Pfeiffer L N and West k W 2002 *Science* **295** 825
[25] Tsukagoshi K, Alphenar B W and Nakazato K 1998 *Appl. Phys. Lett.* **73** 2515
[26] Amlani I, Orlov A O, Snider G L, Lent C S and Bernstein H G 1998 *Appl. Phys. Lett.* **72** 2179
[27] Landauer R 1989 *IBM J. Res. Dev.* **32** 306
[28] Imry Y 1986 *Directions in Condensed Matter Physics* (Singapore: World Scientific)
[29] Buttiker M 1986 *Phys. Rev. Lett.* **57** 1761
[30] Gradshtein I S and Ryzhik 1980 *Tables of Integrals Series and Products* (Academic)
[31] Gurevich V L and Muradov M I unpublished
[32] Tomonaga S 1950 *Prog. Theor. Phys.* **5** 544
Luttinger J M 1963 *J. Math. Phys.* **4** 1154
[33] Emery V J 1979 *Highly Conducting One-Dimensional Solids* (New York: Plenum)
[34] Solyom J 1978 *Adv. Phys.* **28** 201
[35] Schulz H J, Cuniberti G and Pieri P 1997 *Fermi Liquids and Luttinger Liquids (Lecture Notes of the Chia laguna Summer School, Italy)*
[36] Creffield C E, Häusler W and MacDonald A H 2001 *Europhys. Lett.* **53** 221
[37] Häusler W, Kecke L and MacDonald A H 2002 *Phys. Rev.* B **65** 085104
[38] Klesse R and Stern A unpublished
[39] Luther A and Emery V J 1974 *Phys. Rev. Lett.* **33** 589
Chui S T and Lee P A 1975 *Phys. Rev. Lett.* **35** 315
[40] Raichev O E 2001 *Phys. Rev.* B **64** 035324
[41] Muradov M I 2001 *Preprint* cond-mat/0107622
[42] Gurevich V L and Muradov M I 2000 *Phys. Rev.* B **62** 1576
[43] Trauzettel B, Egger R and Grabert H 2002 *Phys. Rev. Lett.* **88** 116401
[44] Mortensen N A, Flensberg K and Jauho A-P 2002 *Phys. Rev.* B **65** 085317
[45] D'Amico I and Vignale G 2002 *Phys. Rev.* B **65** 085109